

Supporting Information

Controlling protein interactions in blood for effective liver immunosuppressive therapy by silica nanocapsules

Shuai Jiang, Domenik Prozeller, Jorge Pereira, Johanna Simon, Shen Han, Sebastian Wirsching, Michael Fichter, Milagro Mottola, Ingo Lieberwirth, Svenja Morsbach, Volker Mailänder, Stephan Gehring, Daniel Crespy, and Katharina Landfester**

Dr. S. Jiang, D. Prozeller, J. Pereira, Dr. J. Simon, S. Han, Dr. I. Lieberwirth, Dr. S. Morsbach,
Prof. V. Mailänder, Dr. D. Crespy, Prof. K. Landfester
Max Planck Institute for Polymer Research
Ackermannweg 10, 55128 Mainz, Germany
E-mail: landfester@mpip-mainz.mpg.de; daniel.crespy@vistec.ac.th

Dr. J. Simon, Prof. V. Mailänder
Dermatology Clinic
University Medical Center of the Johannes Gutenberg-University
Langenbeckstr. 1, 55131 Mainz, Germany

S. Wirsching, Dr. M. Fichter, Prof. S. Gehring
Children's Hospital
University Medical Center of the Johannes-Gutenberg University
Mainz, Germany

M. Mottola
Depto. de Química, Cátedra de Química Biológica
Facultad de Ciencias Exactas, Físicas y Naturales
Universidad Nacional de Córdoba
Av. Vélez Sársfield 1611, X5016GCA Córdoba, Argentina

M. Mottola
CONICET, Instituto de Investigaciones Biológicas y Tecnológicas (IIBYT)
Córdoba, Argentina

Dr. D. Crespy
Department of Materials Science and Engineering
School of Molecular Science and Engineering
Vidyasirimedhi Institute of Science and Technology (VISTEC)
Rayong 21210, Thailand

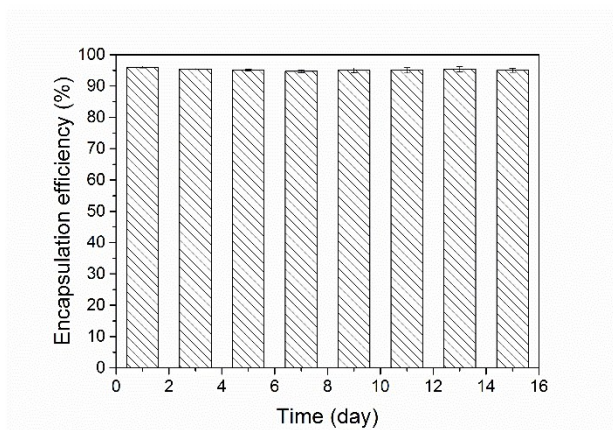


Figure S1. Encapsulation efficiency of DXM in SiO₂ NCs after dialysis for 15 days. The dialysis systems were incubated at 37 °C. Concentrations of DXM in the dialysis media were measured by UV-Vis spectroscopy.

Table S1. Encapsulation efficiency, hydrodynamic diameters D_h , and ζ -potential of SiO₂ NCs loaded with various amounts of DXM and stabilized by CTMA-Cl or Lutensol AT50 (LUT).

Entry	DXM concentration* (mg/mL)		Encapsulation efficiency (%)		D_h (nm)		ζ -potential (mV)
	In olive oil core	In dispersion	UV-vis	HPLC	With CTMA-Cl	With LUT	With LUT
SiO ₂ NCs	0	0	0	0	154 ± 79	158 ± 91	-3.2
SiO ₂ -DXM1 NCs	1	0.03	73.1	76.9	162 ± 73	182 ± 102	-1.3
SiO ₂ -DXM10 NCs	10	0.3	90.6	93.6	160 ± 79	175 ± 99	-2.1
SiO ₂ -DXM50 NCs	50	1.5	94.5	95.3	134 ± 65	151 ± 85	-1.9
SiO ₂ -DXM100 NCs	100	3	96.4	97.0	147 ± 67	159 ± 72	-2.2

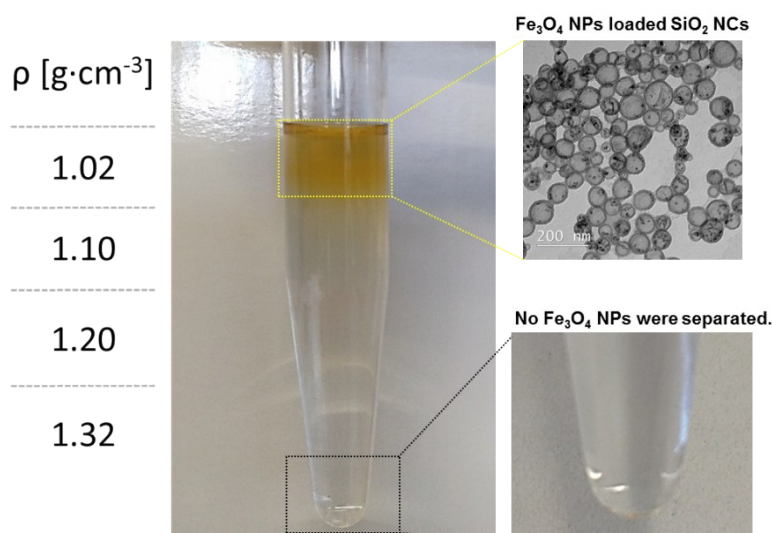


Figure S2. Gradient centrifugation for investigating the encapsulation efficiency of Fe₃O₄ NPs in SiO₂ NCs. Sucrose solutions with densities ranging between 1.00 and 1.30 g·cm⁻³ were prepared (left). The upper brown phase contains Fe₃O₄ NPs labeled SiO₂ NCs (TEM micrograph top right). No solids were collected after the centrifuge process (photograph bottom right), indicating there was no free Fe₃O₄ NPs outside the NCs.

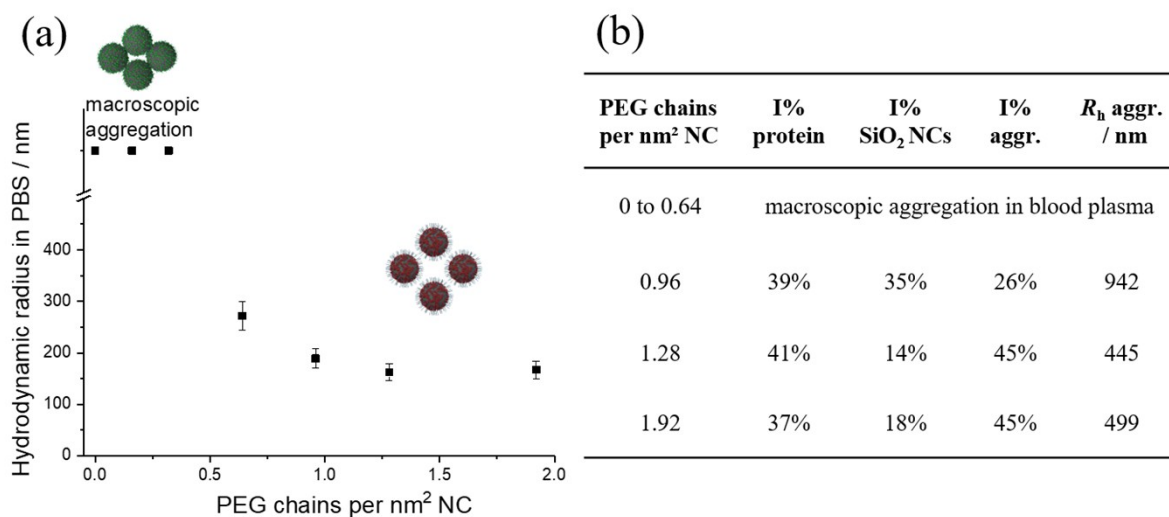


Figure S3. (a) Hydrodynamic radius of PEGylated SiO₂ NCs with various PEGylation density measured with DLS in PBS. (b) Hydrodynamic radius R_h of aggregates formed after incubating SiO₂ NCs in blood plasma with corresponding intensity contribution factors I% of plasma protein, SiO₂ NCs and aggregates (scattering angle 30°, T = 20 °C). Values were determined *via* DLS multicomponent analysis.

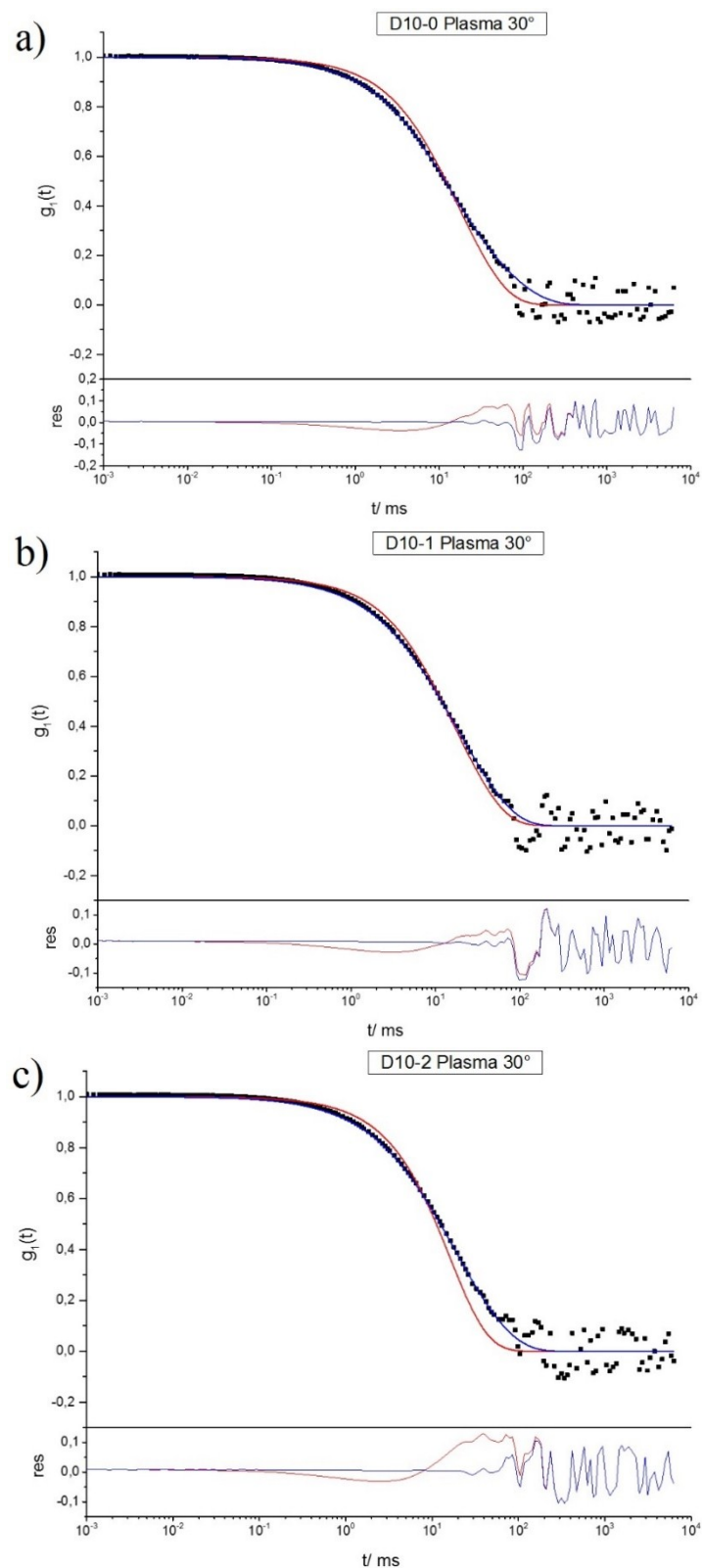


Figure S4. Upper graphs: exemplary autocorrelation functions $g_I(t)$ (black dots) of the mixture of plasma/PEGylated NCs with PEGylation density of (a) 0.96 per nm^2 , (b) 1.28 per nm^2 , and (c) 1.92 per nm^2 at a scattering angle of 30° . Temperature for the measurement was 20°C . The red line represents the fit of the sum of the individual components whereas the blue line represents the fit with an additional aggregation function. Lower graphs: corresponding residuals resulting from the difference between the data and the two fits.

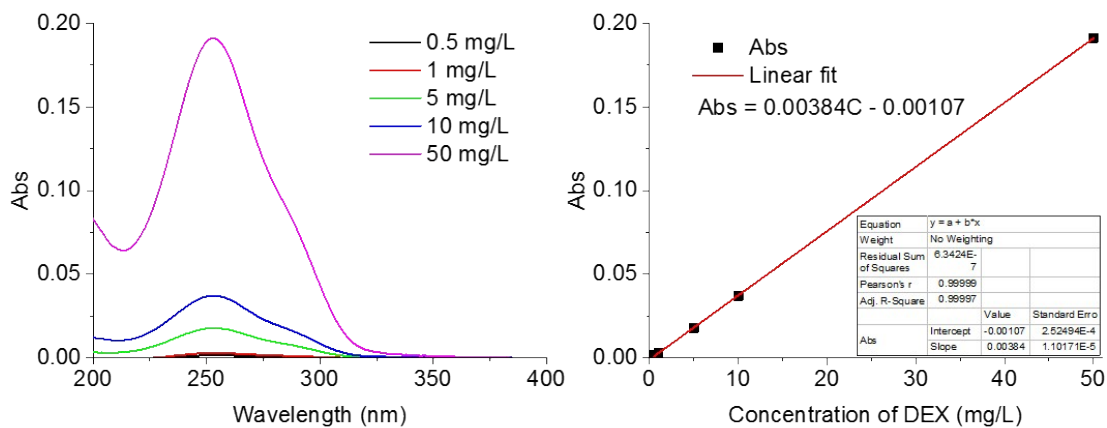


Figure S5. Calibration curve for determining the concentration of DXM in water at pH 7 by UV spectroscopy.